

# Regular nonminimal magnetic black hole as a source of quasiperiodic oscillations

Javlon Rayimbaev<sup>1,2,3,4,†</sup> Ahmadjon Abdujabbarov,<sup>5,1,3,6,4,‡</sup> and Wen-Biao Han<sup>5,7,8,\*</sup>

<sup>1</sup>*Ulugh Beg Astronomical Institute, Astronomy Street 33, Tashkent 100052, Uzbekistan*

<sup>2</sup>*Akfa University, Kichik Halqa Yuli Street 17, Tashkent 100095, Uzbekistan*

<sup>3</sup>*National University of Uzbekistan, Tashkent 100174, Uzbekistan*

<sup>4</sup>*Institute of Nuclear Physics, Ulugbek Street, Tashkent 100214, Uzbekistan*

<sup>5</sup>*Shanghai Astronomical Observatory, 80 Nandan Road, Shanghai 200030, China*

<sup>6</sup>*Tashkent Institute of Irrigation and Agricultural Mechanization Engineers, Kori Niyoziy 39, Tashkent 100000, Uzbekistan*

<sup>7</sup>*School of Fundamental Physics and Mathematical Sciences, Hangzhou Institute for Advanced Study, UCAS, Hangzhou 310024, China*

<sup>8</sup>*School of Astronomy and Space Science, University of Chinese Academy of Sciences, Beijing 100049, China*

(Received 25 March 2021; accepted 5 May 2021; published 28 May 2021; corrected 10 June 2021)

We study the properties of the spacetime around a regular nonminimal magnetic black hole (BH) together with the dynamics of the neutral, magnetized, and magnetically charged particles in its vicinity. The dependence of the values of curvature invariants and the outer event horizon corresponding to the extreme charge of the BH from the coupling parameter are studied in detail. Our study of the test particle motion shows that the innermost stable circular orbit (ISCO) radius decreases with the increase of the magnetic charge of the nonminimal regular magnetic BH. We show that the increase of the ISCO radius with the increase of the coupling parameter is due to the decrease of the extreme value of the BH charge. In particular, when the coupling parameter  $q \rightarrow \infty$  the ISCO radius tends to the value  $r_{\text{ISCO}} = 4.5M$ . The effect of the magnetic charge parameter on ISCO radius can mimic the effect due to the spin parameter of the rotating Kerr BH, and the mimicking values of the spin parameter decreases with the increase of the coupling parameter. We also explore the possible mimicking of the parameters through the observations of twin-peak quasiperiodic oscillations (QPOs). Our analysis shows that the Reissner-Nordström (RN) charge can mimic the spin parameter of the Kerr BH up to  $a/M \simeq 0.51$  provided that there is the same relation between the upper and lower frequencies of the twin-peak QPOs. On the other hand, the nonminimal regular magnetic BH coupling parameter may mimic the spin parameter up to  $a/M \simeq 0.215$  in the relativistic precession model.

DOI: 10.1103/PhysRevD.103.104070

## I. INTRODUCTION

Most astrophysical compact objects are surrounded by the electromagnetic field, and the latter plays an important role in astrophysical processes near compact objects. A weak electromagnetic field around astrophysical black holes (BHs) with a strong gravitational field may not affect the spacetime curvature. However, in some cases when electromagnetic or other fields cannot be considered a test, one needs to consider the coupling of the gravity with additional interactions. On the other hand, there are several

ways of obtaining the theory on where gravity is coupled with other fields. In Scherrer-Jordan-Thiry-Brans-Dicke theory [1–6] the scalar field is coupled (including conformally coupled) to gravity. The most famous model, Einstein-Maxwell theory, considers the nonminimal coupling of gravity and the Maxwell electromagnetic field (see, e.g., Refs. [7–10] for reviews of the theory). In Ref. [11] one may find the review of the Einstein–Yang–Mills theory based on the SU(n) symmetry. The extension of this theory is called as Einstein–Yang–Mills–Higgs models and has been reviewed in [12,13]. In Einstein–Maxwell–axion models the axion pseudoscalar field has been considered as coupled to Einstein–Maxwell field [14].

The BH or other types compact object solutions within nonminimally coupled gravity theories have been obtained in Refs. [15–22]. Particularly, the solutions within the

\*Corresponding author.

wbhan@shao.ac.cn

†javlon@astrin.uz

‡ahmadjon@astrin.uz

Einstein-Yang-Mills theory can be found in Refs. [23–28]. In this paper we will consider the special solution obtained using the Lorentz group symmetry in loop quantum gravity in Einstein-Yang-Mills theory [22,29–32]. We plan to explore the properties of the spacetime and dynamics of test particles while paying attention to the properties of fundamental frequencies.

Since the electromagnetic field is an important part of the spacetime around a compact object, one has to explore the electromagnetic field structure change due to spacetime curvature and the effect of the field on particle dynamics. Particularly interesting is the case in which the particle has a nonzero electric charge or the magnetic moment. In this case the effects of gravity and the electromagnetic field on particle motion can give interesting results and consequences. Within the pure general relativity the properties of the electromagnetic field around BHs in the presence of an external magnetic field have been studied by several authors [33–39]. The effect of the electromagnetic field on charged/magnetized particle dynamics around a BH was explored in Refs. [40–97].

After the first discovery of quasiperiodic oscillations (QPOs) in the power spectra of the flux from x-ray binary pulsars [98] a new direction of study in the physics of accretion disks was opened. QPOs are considered a useful tool in testing the gravity theories describing the BH or other types of compact objects in astrophysics. Current observational data from accretion disks around compact objects give very precise measurements of frequencies of QPOs. This is particularly helpful for checking the different models for astrophysical processes around compact gravitating objects. Observations show that the frequency of QPOs is in the range of 1 mHz to 0.5 kHz. One may distinguish two types of QPOs: low frequency (up to 30 Hz) and high frequency (HF) (up to 500 Hz). HF QPOs observed in BH microquasars have a frequency ratio of around 3:2.

Despite the fact that there is a large number of different models describing the QPOs within the general relativity of alternative theories of gravity, there is still no unique approach to explain the QPOs. However, an interesting point about the characteristic frequencies of HF QPOs is that they are close to the value of those of the test particle, geodesic epicyclic oscillations around the gravitating compact object. Thus, the model of QPOs involving the innermost stable circular orbit (ISCO) of test particles becomes more prominent. This is largely due to the fact that timescales of the orbital motion of the particles near the compact gravitating objects corresponds to the frequencies of QPOs. The so-called relativistic precession model considers QPOs to be the result of motion of accreted inhomogeneities such as blobs or vortices [99–106]. The authors of Refs. [40,103,107–121] assumed that QPOs appear due to the collective motion of matter in either a thin or thick accretion disk.

Here we study the properties of a regular nonminimal magnetic BH through the study of the fundamental frequencies of orbital motion of the particles. The paper is organized as follows: First we explore the spacetime properties around a BH in Einstein-Yang-Mills theory in Sec. II. Section III is devoted to studying the test particle motion while paying attention to circular orbits. In Sec. IV we discuss the fundamental frequencies of orbital motion and apply them to the modeling of the QPOs. We summarize our results in Sec. V. Throughout the paper, we use the system of units where  $G = 1 = c$ . Greek (latin) indices run from 0 (1) to 3.

## II. THE SPACETIME PROPERTIES

The action of the nonminimally coupled Einstein-Yang-Mills theory in four-dimensional spacetimes has the following form [22,31]:

$$\mathcal{S} = \int d^2x \sqrt{-g} \left[ \frac{R}{8\pi} + \frac{1}{2} (F_{\mu\nu} F^{\mu\nu} + \mathcal{R}^{\alpha\beta\mu\nu} F_{\alpha\beta} F_{\mu\nu}) \right], \quad (1)$$

where  $g$  is the determinant of the metric tensor and  $R$  is the Ricci scalar. The Yang-Mills (YM) tensor  $F_{\mu\nu}$  is connected to the YM potential  $A_\mu$  using the following relation:

$$F_{\mu\nu} = \Delta_\mu A_\nu - \Delta_\nu A_\mu + \kappa A_\mu A_\nu, \quad (2)$$

where  $\Delta_\mu$  stands for the covariant derivative and  $\kappa$  is the structure constant parameter of the YM field. Finally, the tensor  $\mathcal{R}^{\alpha\beta\mu\nu}$  has the following form:

$$\begin{aligned} \mathcal{R}^{\alpha\beta\mu\nu} = & -\frac{q}{2} \{ 12R^{\alpha\beta\mu\nu} + g^{\alpha\mu} g^{\beta\nu} - g^{\alpha\nu} g^{\beta\mu} \\ & + R^{\alpha\mu} g^{\beta\nu} - R^{\alpha\nu} g^{\beta\mu} + R^{\beta\nu} g^{\alpha\mu} - R^{\beta\mu} g^{\alpha\nu} \}, \end{aligned} \quad (3)$$

where  $R^{\alpha\beta\mu\nu}$  and  $R^{\alpha\beta}$  are the Riemann and Ricci tensors, respectively, and  $q$  is the nonminimal coupling parameter between the YM and gravitational fields.

The spacetime around magnetically charged regular nonminimal magnetic BHs is described by the line element [22,31,32]

$$ds^2 = -f(r)dt^2 + \frac{1}{f(r)}dr^2 + r^2(d\theta^2 + \sin^2\theta d\phi^2), \quad (4)$$

with the lapse function

$$f(r) = 1 + \left( 1 + \frac{2Q_m^2 q}{r^4} \right)^{-1} \left( -\frac{2M}{r} + \frac{Q_m^2}{r^2} \right), \quad (5)$$

where  $M$  and  $Q_m$  are the total mass and the magnetic charge of the BH. The electromagnetic field four-potential of the nonrotating regular nonminimal magnetic BH reads

$$A_\alpha = (0, 0, 0, Q_m \cos \theta). \quad (6)$$

In fact, when  $q = 0$  the spacetime metric (5) reduces to spacetime around the magnetically charged Reissner-Nordström BH.

### A. Scalar invariants

A detailed analysis of curvature invariants such as the Ricci scalar, square of the Ricci tensor, and the Kretschmann scalar may result in a deep understanding of the main properties of the spacetime. For that reason in this subsection we investigate the curvature invariants of the spacetime metric (4).

#### 1. The Ricci scalar

First, we explore the effects of the spacetime parameters on the value of the Ricci scalar. The expression for the Ricci scalar can be easily found in the following form:

$$\begin{aligned} R &= g^{\mu\nu} R_{\mu\nu} \\ &= \frac{8qQ_m^2}{(2qQ_m^2 + r^4)^3} [5Q_m^2 r(4Mq + r^3) - 6(qQ_m^4 - Mr^5)]. \end{aligned} \quad (7)$$

One can see from Eq. (7) that in the Schwarzschild limit it takes the form

$$\lim_{r \rightarrow 0} R = -\frac{6}{q}. \quad (8)$$

From Eq. (7) one may also see that

$$\lim_{q \rightarrow 0} R = \lim_{q \rightarrow \infty} R = 0. \quad (9)$$

#### 2. The square of the Ricci tensor

Now we explore the square of the Ricci tensor for spacetime (4), which can be found in the following form:

$$\begin{aligned} R_{\mu\nu} R^{\mu\nu} &= \frac{4Q_m^4}{(2qQ_m^2 + r^4)^6} \{28qr^{12}(2Mr - Q_m^2) + r^{16} \\ &\quad - 16q^3Q_m^2r^4(15Q_m^2 - 22Mr)(Q_m^2 - 4Mr) \\ &\quad + 8q^2r^8(116M^2r^2 - 130MQ_m^2r + 37Q_m^4) \\ &\quad + 16q^4(104M^2Q_m^4r^2 - 60MQ_m^6r + 9Q_m^8)\}. \end{aligned}$$

One can easily see that in the limiting cases it has the following form:

$$\lim_{q \rightarrow 0} R_{\mu\nu} R^{\mu\nu} = \frac{4Q_m^4}{r^8}, \quad \lim_{q \rightarrow \infty} R_{\mu\nu} R^{\mu\nu} = 0. \quad (10)$$

The square of the Ricci tensor (10) vanishes as the parameter  $q$  tends to zero, and for the nonzero values of  $q$  parameter it has the following form:

$$\lim_{r \rightarrow 0} R_{\mu\nu} R^{\mu\nu} = \frac{9}{q^2}. \quad (11)$$

#### 3. The Kretschmann scalar

Now we explore the Kretschmann scalar, which gives more information about the properties of the curvature of the spacetime (4). Since the Kretschmann scalar does not vanish even for Ricci flat spacetime, it is helpful to study the properties of a given Ricci flat spacetime. The exact analytic expression for the Kretschmann scalar for the spacetime (4) has the form

$$\begin{aligned} K &= \frac{8}{(2qQ_m^2 + r^4)^6} \{r^{16}(6M^2r^2 - 12MQ_m^2r + 7Q_m^4) \\ &\quad - 16q^4Q_m^8(38M^2r^2 - 20MQ_m^2r + 3Q_m^4) \\ &\quad + 4qQ_m^2r^{12}(24M^2r^2 - 48MQ_m^2r + 17Q_m^4) \\ &\quad - 16q^3Q_m^6r^4(56M^2r^2 - 40MQ_m^2r + 5Q_m^4) \\ &\quad + 8q^2Q^4r^8(154M^2r^2 - 152MQ_m^2r + 37Q_m^4)\}. \end{aligned} \quad (12)$$

The limits of the and in the Kretschmann scalar have the following forms:

$$\lim_{r \rightarrow 0} K = \frac{6}{q^2}, \quad (13)$$

$$\lim_{q \rightarrow 0} K = \frac{8}{r^8}(6M^2r^2 - 12MQ_m^2r + 7Q_m^4), \quad (14)$$

$$\lim_{q \rightarrow \infty} K = 0. \quad (15)$$

Figure 1 demonstrates the radial dependence of the Ricci scalar, the square of the Ricci tensor, and the Kretschmann scalar of the spacetime (4) for the different values of the nonminimal coupling parameter and the fixed magnetic charge of the nonminimal regular magnetic BH. One can see that all the spacetime invariants decrease with an increase of the nonminimal coupling parameter.

### B. Event horizon

Here we aim to show detail analysis of the exploration of the event horizon properties of the regular nonminimal magnetic BH spacetime governed by the lapse function given in Eq. (5) as a function of the nonminimal parameters  $q$  and the regular BH charge  $Q_m$ .

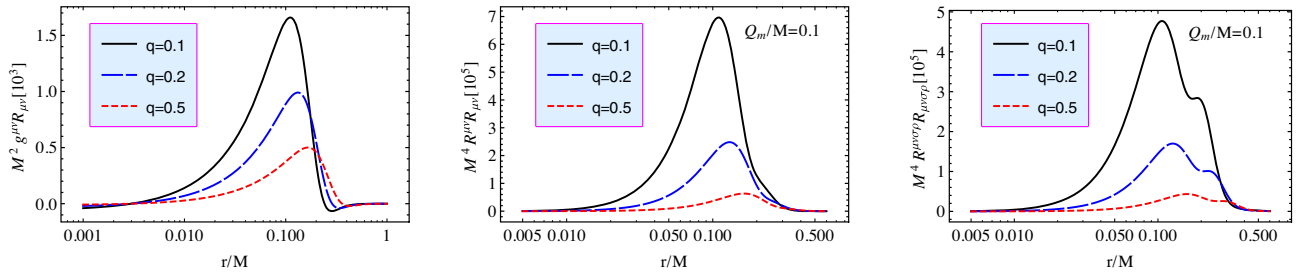


FIG. 1. Radial profiles of scalar invariants of the spacetime (4) for the different values of the nonminimal parameter  $q$  and the fixed magnetic charge of the BH  $Q_m/M = 0.1$ . The left, middle, and right panels correspond to the radial dependence of the Ricci scalar, Ricci tensor, and Kretschmann scalar, respectively.

The radius of the event horizon of a BH corresponds to the case in which  $g_{rr} \rightarrow \infty$ ,  $g^{rr} = 0$ , namely, the solution of the equation

$$f(r) = 0, \quad (16)$$

and we have

$$\left(\frac{r_h}{M}\right)_\pm = 1 + Y_1 \pm \left\{ 2 + \frac{2}{Y} - \frac{Y_1}{3\sqrt[3]{2}M^2} - \frac{Q_m^2}{M^2} \left( \frac{4}{3} - \frac{2}{Y} + \frac{\sqrt{3}2(24q + Q_m^2)}{3Y_1} \right) \right\}^{\frac{1}{2}}, \quad (17)$$

where

$$\begin{aligned} \frac{1}{2}Y^3 &= 108M^2qQ_m^2 - 72qQ_m^4 + Q_m^6 \\ &\quad + \sqrt{(108M^2qQ_m^2 - 72qQ_m^4 + Q_m^6)^2 - (24qQ_m^2 + Q_m^4)^3}, \\ Y_1^2 &= 1 - \frac{2Q_m^2}{3M^2} + \frac{Y_1}{3\sqrt[3]{2}} + \frac{\sqrt[3]{2}Q_m^2}{3Y_1}(24q + Q_m^2), \end{aligned} \quad (18)$$

and where  $\pm$  stands for the outer and inner horizons.

One can see the effects of the nonminimal coupling parameters  $q$  and the BH charge  $Q_m$  on the event horizon [Eq. (17)] is a quite complicated form to see. By the wa, we show plots of Eq. (17) for the different values of the coupling parameter  $q$ .

The dependence of the event horizon of the regular nonminimal magnetic BH from the BH charge is shown in Fig. 2 for different values of the nonminimal coupling parameter. One can see from the figure that there is an extreme value for the BH charge in which the two roots of the equation  $f(r) = 0$  match and BH does not exist for  $Q > Q_{\text{extr}}$ . The extreme charge of the BH decreases as the parameter grows, and at larger values of the magnetic charge of the BH the coupling parameter is weakened while the radius of the event horizon increases. The dependence of the extreme values of the BH charge and minimal value of the outer event horizon from the nonminimal coupling parameter is shown in Fig. 3.

Now we will analyze the extreme charge of the BH and minimal (maximal) value of the outer (inner) horizon by setting the following system of equations and solving them with respect to  $r$  and  $Q_m$ :

$$f(r) = 0 = f'(r), \quad (19)$$

and immediately we have

$$\frac{3(r_h)_{\min}}{M} = 1 + X + X^{-1}(1 - 12q) \quad (20)$$

$$\begin{aligned} \frac{3Q_{\text{extr}}^2}{M^2} &= X^{-2}\{1 - 96q^2 + q(16X^2 - 62X + 121) \\ &\quad + X^2 + X - 2XX_1 + 5X_1\}, \end{aligned} \quad (21)$$

where

$$X^3 = 1 + 3(21q + X_1), \quad X_1^2 = 3q(q + 2)(64q + 3). \quad (22)$$

One may see the effect of the coupling parameter  $q$  on the extreme value of the magnetic BH and the minimal value of its outer horizon using Eqs. (20) and (21).

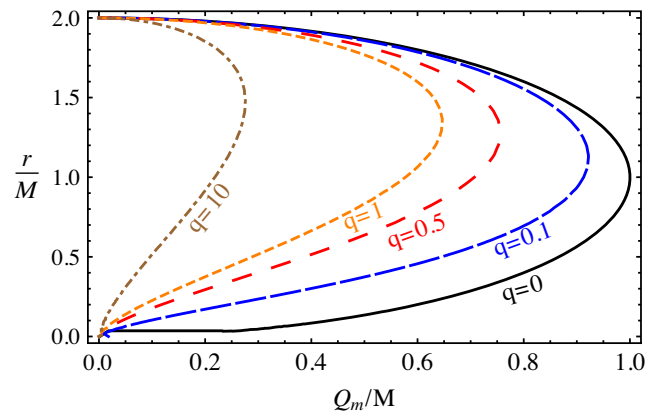


FIG. 2. Dependence of the event horizon radius on the magnetic charge of the regular magnetic BH,  $Q_m$ , for different values of the nonminimal coupling parameter  $q$ .  $q/M^2$  is presented as  $q$ .

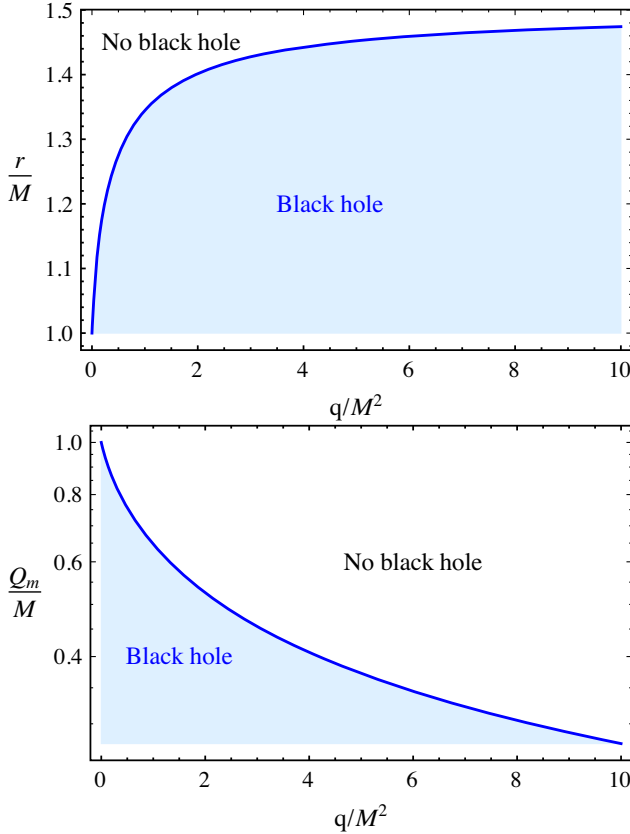


FIG. 3. Dependence of (top panel) the minimum value of the outer (event) horizon radius and (bottom panel) the maximum value of the magnetic charge  $Q_m$ , which allows the BH to exist, on the nonminimal coupling parameter  $q$ .

The dependence of the extreme value of the BH charge and minimum value of the horizon from the coupling parameter  $q$  is presented in Fig. 3. One can see from Fig. 3 that when the nonminimal coupling parameter  $q = 0$  [pure RN BH case] the extreme value of the charge and the minimal value of the event horizon are equal to  $Q_{\text{extr}} = (r_h)_{\min} = M$ . One may see that the minimal value of the event horizon increases with an increase of the coupling parameter, while the extreme charge decreases. The limits of the minimal outer horizon and the magnetic charge of the magnetic BH at an infinite value of the coupling parameter are

$$\lim_{q \rightarrow \infty} \frac{r_{\min}}{M} = \frac{3}{2}, \quad \lim_{q \rightarrow \infty} \frac{Q_{\text{extr}}}{M} = 0. \quad (23)$$

Figure 4 shows the radial dependence of the lapse function of the extreme charged regular nonminimal magnetic BH for different values of the nonminimal coupling parameter.

### III. TEST PARTICLE MOTION

In this section we investigate the test particle dynamics in the spacetime (4) around regular magnetic BHs.

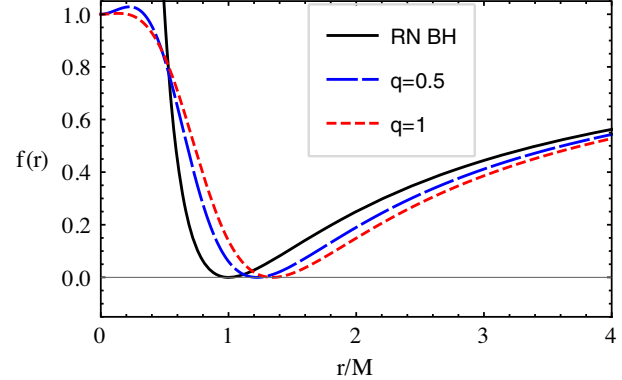


FIG. 4. The radial dependence of lapse function for the different values of the nonminimal parameter and the corresponding values of the magnetic charge  $Q_m \rightarrow Q_{\text{extr}}$ .

#### A. Equation of motion

Consider the dimensionless Lagrangian density for a neutral particle with mass  $m$ :

$$\mathcal{L}_p = \frac{1}{2} g_{\mu\nu} \dot{x}^\mu \dot{x}^\nu. \quad (24)$$

Note that the magnetic charge of the regular nonminimal magnetic BH does not interact with the test neutral particle. The two conserved quantities, the specific energy  $\mathcal{E} = E/m$  and the specific angular momentum of the particle  $\mathcal{L} = L/m$ , are defined as

$$g_{tt} \dot{t} = -\mathcal{E}, \quad g_{\phi\phi} \dot{\phi} = \mathcal{L}. \quad (25)$$

The equation of motion for a test particle can be governed by the standard normalization condition

$$g_{\mu\nu} u^\mu u^\nu = \epsilon, \quad (26)$$

where  $\epsilon$  has the values 0 and  $-1$  for massless and massive particles, respectively.

For the massive neutral particles the motion is governed by timelike geodesics of the spacetime (4), and the equations of motion can be found using Eq. (26). Taking Eq. (25) into consideration, one may easily obtain the equation of motion in the form

$$\dot{r}^2 = \mathcal{E}^2 + g_{tt} \left( 1 + \frac{\mathcal{K}}{r^2} \right), \quad (27)$$

$$\dot{\theta} = \frac{1}{g_{\theta\theta}^2} \left( \mathcal{K} - \frac{\mathcal{L}^2}{\sin^2 \theta} \right), \quad (28)$$

$$\dot{\phi} = \frac{\mathcal{L}}{g_{\phi\phi}}, \quad (29)$$

$$\dot{t} = -\frac{\mathcal{E}}{g_{tt}}, \quad (30)$$

where  $\mathcal{K}$  denotes the Carter constant.

Restricting the motion of the particle to the equatorial plane, in which  $\theta = \pi/2$  and  $\dot{\theta} = 0$ , the Carter constant takes the form  $\mathcal{K} = \mathcal{L}^2$  and the equation of the radial motion can be expressed in the form

$$\dot{r}^2 = \mathcal{E}^2 - V_{\text{eff}}, \quad (31)$$

where the effective potential of the motion of neutral particles at the equatorial plane reads

$$V_{\text{eff}} = f(r) \left( 1 + \frac{\mathcal{L}^2}{r^2} \right). \quad (32)$$

Now one may consider the conditions for the circular motion, which indicate that there is no radial motion ( $\dot{r} = 0$ ) and no acceleration in the radial direction ( $\ddot{r} = 0$ ). One may easily obtain the radial profiles of the specific angular momentum and a specific energy for circular orbits at the equatorial plane ( $\theta = \pi/2$ ) in the following form:

$$\mathcal{L}^2 = \frac{r^4}{\mathcal{Z}(r)} [2qQ_m^4 + Mr^5 - Q_m^2(6Mqr + r^4)], \quad (33)$$

$$\mathcal{E}^2 = \frac{1}{\mathcal{Z}(r)} [Q_m^2(2q + r^2) + r^3(r - 2M)]^2, \quad (34)$$

where

$$\mathcal{Z}(r) = 2r^3Q_m^2(Mq + 2qr + r^3) + 4q^2Q_m^4 + r^7(r - 3M). \quad (35)$$

Figure 5 demonstrates the radial dependence of the specific energy and angular momentum of test particles around regular nonminimal BHs for different values of the coupling parameter  $q$  and fixed value of the magnetic charge  $Q_m/M = 0.8$  compared to the Schwarzschild and RN BHs. One can see from Fig. 5 that the existence of the BH charge and the coupling parameter cause a decrease of the minimum value in both specific angular momentum and energy of the particle and the distance where the energy and angular momentum take the minimal values.

We show the dependence of the minimal radius of circular orbits from the magnetic charge of the nonminimal magnetic BH for different values of the coupling parameter compared to the RN BH case in Fig. 6. One can easily see from Fig. 6 that the increase of the magnetic charge of the BHs causes a decrease of the radius and a decrease of the rate of the minimal radius growth at higher values of the nonminimal coupling parameter.

## B. Innermost stable circular orbits

The standard way to get the radius of ISCOs is to solve the inequality governed by the condition  $\partial_{rr}V_{\text{eff}} \geq 0$ . Using the expression for the effective potential one may obtain the following algebraic inequality:

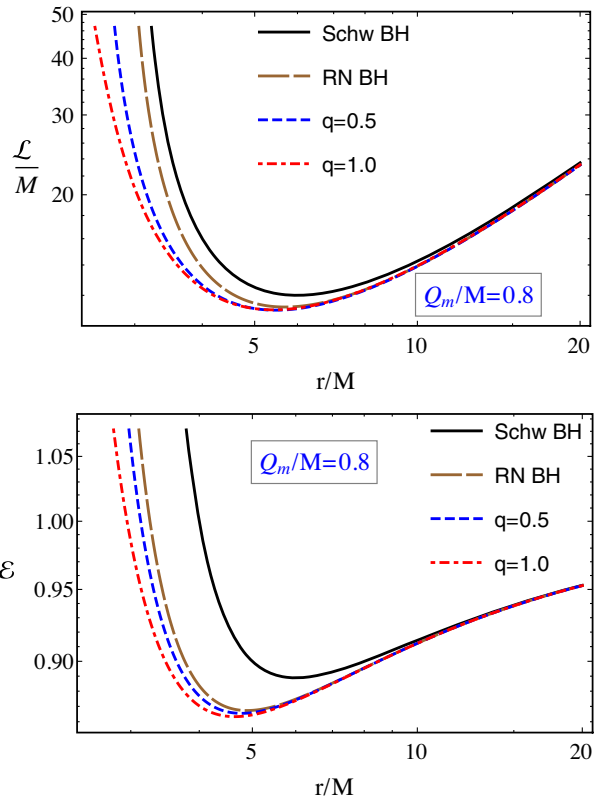


FIG. 5. The radial dependence of (top panel) specific angular momentum and (bottom panel) energy for circular orbits for different values of the nonminimal coupling parameter  $q$  than the Schwarzschild and RN BH cases.

$$\begin{aligned} & 2qr^3Q_m^2[MQ_m^2 + 18Mr^2 - 6r(2Q_m^2 + M^2)] \\ & + r^6[9MrQ_m^2 - 4Q_m^4 + Mr^2(r - 6M)] \\ & + 4q^2(4Q_m^6 - 15MrQ_m^4) \geq 0. \end{aligned} \quad (36)$$

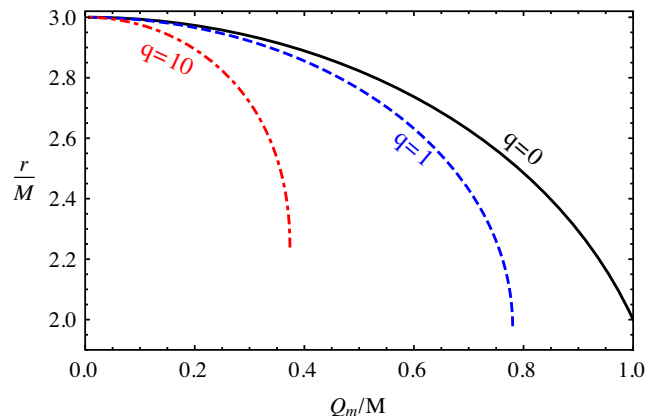


FIG. 6. Dependence of the minimal distance where circular motion is allowed from the magnetic charge of the regular nonminimal BH for different values of the nonminimal coupling parameter ( $q/M^2 \rightarrow q$ ).

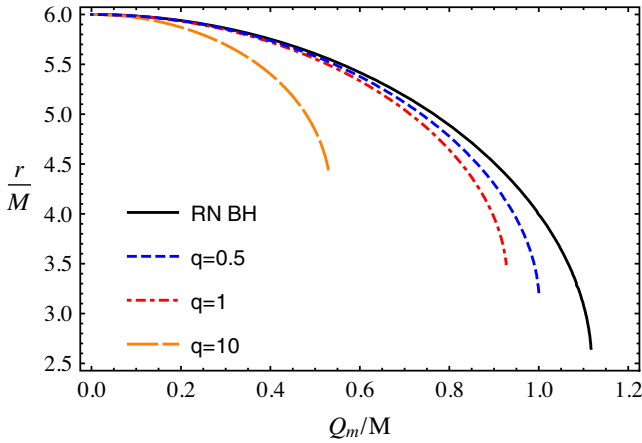


FIG. 7. Dependence of the ISCO radius of the neutral massive particles around a regular nonminimal magnetic BH from the magnetic charge of the BH for different values of the nonminimal coupling parameter compared to the RN case.

The exact solutions of Eq. (36) in the limiting case in which  $q$  tends to infinity and 0, respectively, have the following form:

$$\lim_{q \rightarrow \infty} \frac{r_{\text{ISCO}}}{M} = \frac{9}{2}, \quad \lim_{q \rightarrow 0} \frac{r_{\text{ISCO}}}{M} = 4. \quad (37)$$

Figure 7 demonstrates the dependence of the ISCO radius of the test particles from the magnetic charge of the nonminimal magnetic BH for different values of the coupling parameter compared to the RN BH. One can see that the increase of the magnetic charge of the BH causes the decrease of the ISCO radius, and the minimum value of the ISCO radius corresponding to the extremely charged BH case increases with an increase of the coupling parameter. Moreover, the ISCO radius of test particles decreases faster in the case of regular nonminimal magnetic BHs than in the RN BH.

### C. Regular nonminimal magnetic BH versus Kerr BH

In the previous subsection we found that the existence of BH charge causes a decrease in the ISCO radius of test particles. On the other hand, the effect of the spin parameter and the charge of the BH on the ISCO radius are similar, and it will be difficult to distinguish them using the measurements of the ISCO radius from astronomical observations. In this subsection, we explore the degeneracy problem of the effect of magnetic charge  $Q_m$  of the regular nonminimal magnetic BH and the spin of the Kerr BH on the ISCO radius. We discuss how to distinguish the BHs through (direct or indirect) measurements of the ISCO radius.

The expression for the ISCO radius of test particles around rotating Kerr BHs with the spin parameter  $a$  for retrograde and prograde orbits has the following form [122]:

$$r_{\text{ISCO}} = 3 + Z_2 \pm \sqrt{(3 - Z_1)(3 + Z_1 + 2Z_2)}, \quad (38)$$

with

$$Z_1 = 1 + (\sqrt[3]{1+a} + \sqrt[3]{1-a})^3 \sqrt{1-a^2},$$

$$Z_2^2 = 3a^2 + Z_1^2.$$

Figure 8 illustrates the relation between spin and the magnetic charge of the BH. One can see from Fig. 8 that the RN BH charge can mimic the spin of a rotating Kerr BH up to  $a/M = 0.4899$  (the result is compatible with the previous results of Refs. [92,96]), while the charge of the regular nonminimal magnetic BH can reflect the same gravitational effects due to the spin of the Kerr BH up to  $a/M = 0.3936$  corresponding to the value of the coupling parameter  $q = 1$ . This maximal mimicking value decreases with the increase of the coupling parameter and takes the value  $a/M = 0.3271$  for  $q = 10$ . In our previous work [92] we showed that the charge of a regular BH in general relativity combined to the nonlinear electrodynamics can mimic the spin of a rotating Kerr BH up to  $a/M = 0.8$ , while the charge of a BH in Einstein-Maxwell-scalar gravity can mimic up to  $a/M = 0.936$  [95]. The charge of a regular Bardeen BH may mimic the spin parameter of the Kerr BH up to  $a/M = 0.9$  [80] and the charge of a deformed RN BH with the deformation parameter  $\epsilon = 6.17$  up to  $a/M = 0.88$  [96].

### D. The energy efficiency

According to the Novikov-Thorne model [123], the Keplerian accretion around an astrophysical BH is modeled as geometrically thin disks governed by the properties of the spacetime circular geodesics. Generally, the energy efficiency of the accretion disk around a BH indicates the maximum energy which can be extracted as radiation of the infalling matter into the central BH. The efficiency of

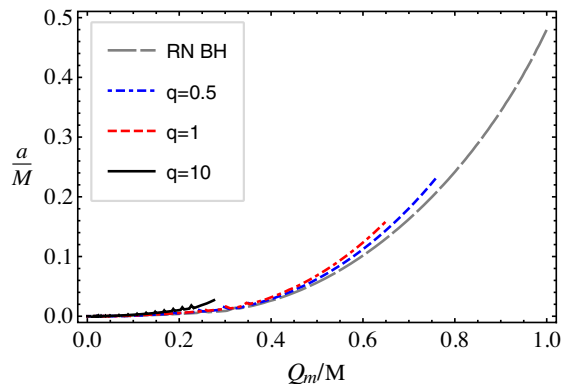


FIG. 8. The degeneracy relations between the spin of the Kerr BH and the magnetic charge of the magnetic regular BH providing the same value of the ISCO radius for different values of the nonminimal coupling parameter  $q$ .

the accreting test particle can be calculated through the following expression:

$$\eta = 1 - \mathcal{E}|_{r=r_{\text{ISCO}}}, \quad (39)$$

where  $\mathcal{E}|_{r=r_{\text{ISCO}}}$  is the binding energy of the particle at the ISCO normalized to the rest energy of the test particle.  $\mathcal{E}|_{r=r_{\text{ISCO}}}$  can be calculated using the energy of the particles given by Eq. (33) at ISCO. The exact analytical form of the efficiency is hard to obtain due to the complicated form of the ISCO radius. The effects of the magnetic charge of regular nonminimal magnetic BH and nonminimal coupling parameters on the efficiency are calculated numerically, and results are shown in Fig. 9 compared to the energy efficiency of the RN BH. From Fig. 9 one can easily see that the value of the energy efficiency decreases with the increase in the nonminimal coupling parameter due to the decrease in the extreme charge of the BH.

The energy efficiency from a BH has another important astrophysical application connected with bolometric luminosity of the accretion disk through the relation  $L_{\text{bol}} = \eta \dot{M} c^2$ , where  $\dot{M}$  is the mass rate of accretion matter into the central BH. The bolometric luminosity can be obtained through observations, and here we will discuss the problem regarding how the BH charge can mimic the spin of the Kerr BH providing that there is the same value for the energy efficiency/bolometric luminosity.

One can see from Fig. 10 that the magnetic charge of the RN BH can mimic the spin of the Kerr BH up to  $a/M = 0.5079$ , and it is significantly stronger than the mimicking value obtained using the measurements of the ISCO radius. Moreover, an increase in the coupling parameter causes a decrease in the mimicking value. Since the YM field increases the effect of the magnetic charge of the BH relative to the charge of the RN BH, one may conclude that it is possible to distinguish the regular nonminimal magnetic BH from the RN one only for large values of the magnetic charge.

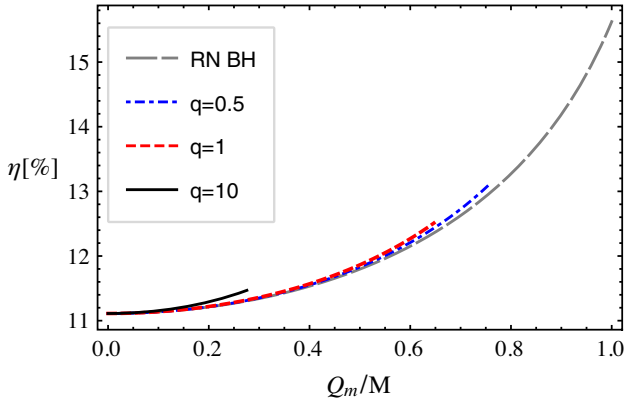


FIG. 9. Dependence of the energy efficiency from the magnetic charge of the regular nonminimal magnetic BH for different values of the nonminimal coupling parameter  $q$ .

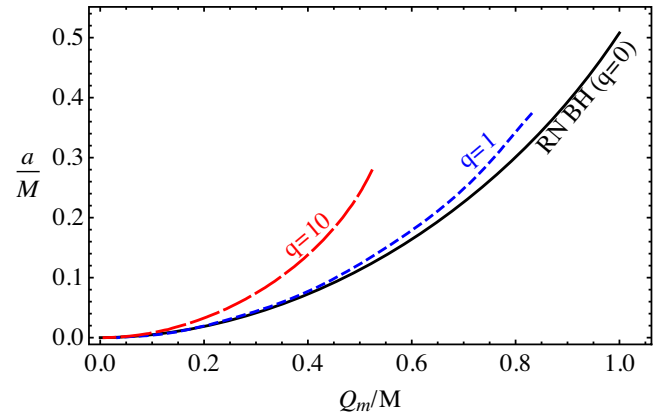


FIG. 10. Degeneracy relations between the spin of a rotating Kerr BH and the magnetic charge of the regular nonminimal magnetic BH providing the same value of energy efficiency for different values of the nonminimal coupling parameter  $q$ .

#### IV. FUNDAMENTAL FREQUENCIES

For a spherically symmetric spacetime, there are two fundamental frequencies of test particle motion. One is the  $\Omega_r$  corresponding to the radial coordinate  $r$ , which goes from the periastron to the apastron and back to the periastron. However, because of the perihelion precession, the particle will go more than  $2\pi$  in the azimuthal direction. Therefore, we will have another orbital frequency  $\Omega_\phi$ . Here we explore the fundamental frequencies in spacetime around a nonminimal magnetic BH.

##### A. Keplerian frequency

The angular velocity for a distant observer or so-called Keplerian frequency is determined as

$$\Omega_K = \frac{d\phi}{dt} = \frac{\dot{\phi}}{t}. \quad (40)$$

One may rewrite Eq. (40) for the spacetime metric (4) and obtain the following form for the Keplerian frequency:

$$\begin{aligned} \Omega_K &= \sqrt{\frac{f'(r)}{2r}} \\ &= \frac{\sqrt{2qQ^2(Q^2 - 3Mr) - r^4(Q^2 - Mr)}}{2qQ^2 + r^4}. \end{aligned} \quad (41)$$

To compare the fundamental frequencies to the corresponding astrophysical quantities, we will express them in units of hertz using the relation

$$\nu = \frac{1}{2\pi} \frac{c^3}{GM} \Omega \text{ [Hz]}. \quad (42)$$

The radial dependence of the Keplerian frequencies of test particles around a nonminimal regular BH shown in

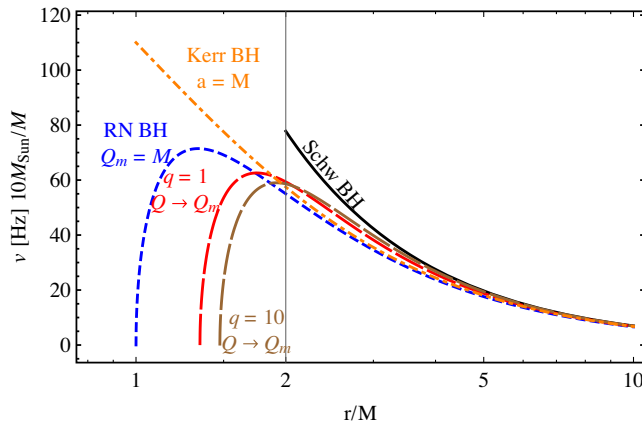


FIG. 11. Radial dependence of the Keplerian frequencies of test particles around an extreme rotating Kerr BH and extremely charged RN and nonminimal magnetic BHs for different values of the nonminimal coupling parameter  $q$ .

Fig. 11 in comparison with the Kerr BH case [124,125]. To compare the effects of the nonminimal regular BH charge and the coupling parameter we have provided the Keplerian frequencies of the test particles around the Schwarzschild, extreme charge RN, and extreme rotating Kerr BHs. From Fig. 11 one can easily see that in the presence of a YM field the maximum of the frequency is decreasing.

### B. Harmonic oscillations

In this subsection we provide an analysis of the fundamental frequencies governed by test neutral particle motion around a nonminimal regular magnetic BH. The radial and vertical fundamental frequencies can be calculated by considering small perturbations along the radial  $r \rightarrow r_0 + \delta r$  and vertical  $\theta \rightarrow \theta_0 + \delta\theta$  directions, respectively, around the circular orbit. The effective potential can be expanded in terms of  $r$  and  $\theta$  in the form

$$\begin{aligned} V_{\text{eff}}(r, \theta) = & V_{\text{eff}}(r_0, \theta_0) + \delta r \partial_r V_{\text{eff}}(r, \theta)|_{r_0, \theta_0} \\ & + \delta \theta \partial_\theta V_{\text{eff}}(r, \theta)|_{r_0, \theta_0} + \frac{1}{2} \delta r^2 \partial_r^2 V_{\text{eff}}(r, \theta)|_{r_0, \theta_0} \\ & + \frac{1}{2} \delta \theta^2 \partial_\theta^2 V_{\text{eff}}(r, \theta)|_{r_0, \theta_0} \\ & + \delta r \delta \theta \partial_r \partial_\theta V_{\text{eff}}(r, \theta)|_{r_0, \theta_0} + \mathcal{O}(\delta r^3, \delta \theta^3). \end{aligned} \quad (43)$$

Careful analysis of the expansion (43) shows that the first term of Eq. (43) vanishes due to the condition  $\partial_r V_{\text{eff}} = 0$ . On the other hand, using the stability conditions of the effective potential in Eq. (32) one can remove the second, third, and last terms. Finally, only two terms proportional to the second order derivatives from the effective potential with respect to  $r$  and  $\theta$  remain. To get physical quantities measured by a distant observer in the equation of motion, we replace a derivation with respect to the affine parameter

with the time derivation ( $dt/d\lambda = u^t$ ). Substituting Eq. (43) into Eq. (32) and taking into account the aforementioned assumptions, one may easily obtain harmonic oscillator equations for displacements  $\delta r$  and  $\delta\theta$  in the form

$$\frac{d^2 \delta r}{dt^2} + \Omega_r^2 \delta r = 0, \quad \frac{d^2 \delta\theta}{dt^2} + \Omega_\theta^2 \delta\theta = 0. \quad (44)$$

The quantities  $\Omega_r$  and  $\Omega_\theta$  in Eq. (44) are the radial and vertical angular frequencies measured by a distant observer, respectively, and defined as

$$\Omega_r^2 = -\frac{1}{2g_{rr}t^2} \partial_r^2 V_{\text{eff}}(r, \theta)|_{\theta=\pi/2}, \quad (45)$$

$$\Omega_\theta^2 = -\frac{1}{2g_{\theta\theta}t^2} \partial_\theta^2 V_{\text{eff}}(r, \theta)|_{\theta=\pi/2}, \quad (46)$$

$$\Omega_\phi = \frac{d\phi}{dt}. \quad (47)$$

Finally, the radial and vertical frequencies in spacetime of a regular nonminimal magnetic BH will have the form

$$\begin{aligned} \Omega_r = \Omega_K \left\{ 1 + \frac{2Q^2(8q + r^2)}{2qQ^2 + r^4} \right. \\ \left. + \frac{r^2(6M^2r^2 - Q^2r(7M + r) + 2Q^4)}{r^4(Q^2 - Mr) - 2q(Q^4 - 3MQ^2r)} \right. \\ \left. + \frac{2q(5Q^4 - 12MQ^2r)}{r^4(Q^2 - Mr) - 2q(Q^4 - 3MQ^2r)} \right\}^{\frac{1}{2}}, \end{aligned} \quad (48)$$

$$\Omega_\theta = \Omega_\phi = \Omega_K. \quad (49)$$

Figure 12 shows the radial dependence of the radial frequencies of test particles around nonminimal regular magnetic BHs for different values of the coupling parameter  $q$  compared to the corresponding frequencies around a

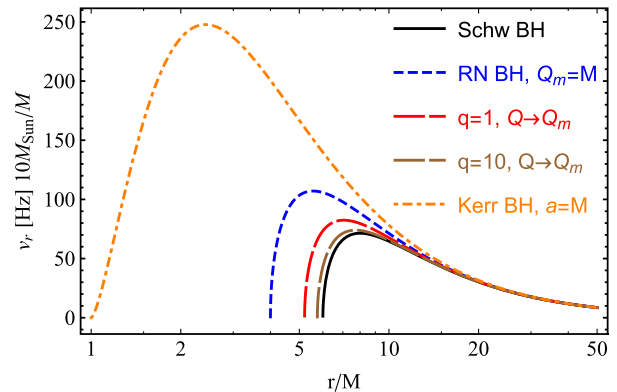


FIG. 12. Radial dependence of frequencies of radial oscillations of test particles around an extreme Kerr BH and extremely charged RN and nonminimal magnetic BHs for different values of the nonminimal coupling parameter  $q$ .

Schwarzschild BH, an extremely charged RN BH, and an extreme rotating Kerr BH. From Fig. 12 one can easily see that the maximum value of the radial frequency decreases due to an increase in the coupling parameter of the YM field, while it increases with an increase in the BH charge and the spin of a rotating Kerr BH. The distance where the frequency takes its maximum decreases with an increase in the spin and charge parameters of the Kerr and RN BHs, respectively. On the other hand, an increase of the coupling parameter causes the distance where the frequency takes its maximum to slightly increase.

### C. Regular magnetic BH versus Kerr BH: The same frequencies of QPO

In this subsection we will discuss the possible frequencies of various models of twin-peak QPOs around a BH in the presence of a YM field compared to those around Schwarzschild, RN, and Kerr BHs [126]. In most cases, twin QPO models tell one that the role of the gravitational field of the central BH is crucial and that frequencies of the oscillation depend on the frequencies of harmonic oscillations along the geodesic orbits. Here we analyze the relations between possible values of low and high

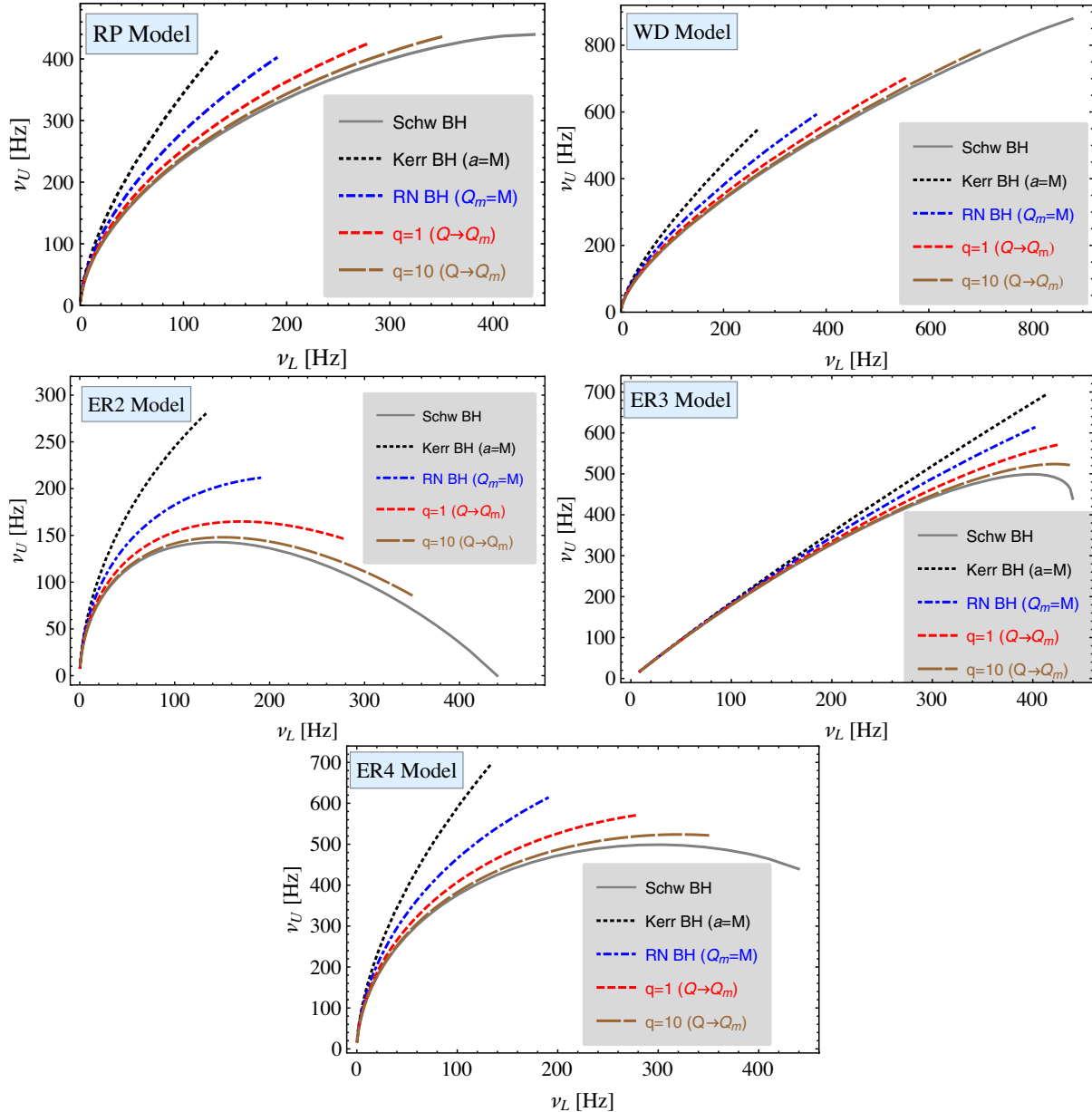


FIG. 13. Relations between the frequencies of upper and lower picks of twin-peak QPOs in the RP, WD, and ER2–ER4 models around a Schwarzschild BH, an extremely rotating Kerr BH, and extremely charged RN and nonminimal magnetic BHs for different values of the nonminimal coupling parameter  $q$ .

frequencies of twin-peak QPOs around a central BH for different values of parameters of the central object. In particular, we will explore the following QPO models:

- (a) Relativistic precession (RP) model [127]. In the standard RP model the upper and lower frequencies are identified through the radial and orbital frequencies as  $\nu_U = \nu_\phi$  and  $\nu_L = \nu_\phi - \nu_r$ , respectively. In modified RP1 and RP2 models the frequencies can be identified as  $\nu_U = \nu_\theta$ ,  $\nu_L = \nu_\phi - \nu_r$  and  $\nu_U = \nu_\phi$ ,  $\nu_L = \nu_\theta - \nu_r$ , respectively.
- (b) The epicyclic resonance (ER2, ER3, ER4) models [103]. In the ER models the accretion disk is assumed to be thick enough and QPO appears due to the resonance oscillations of uniformly radiating particles along the geodesic orbits. The upper and lower frequencies for the ER2, ER3, and ER4 models are defined through frequencies of orbital and epicyclic oscillations as  $\nu_U = 2\nu_\theta - \nu_r$ ,  $\nu_L = \nu_r$ ,  $\nu_U = \nu_\theta + \nu_r$ ,  $\nu_L = \nu_\theta$  and  $\nu_U = \nu_\theta + \nu_r$ ,  $\nu_L = \nu_\theta - \nu_r$ , respectively.
- (c) The warped disk (WD) model [128,129]. In the WD model the QPO frequencies appear to be due to the oscillation of the warped thin disk. The upper and lower frequencies are defined as  $\nu_U = 2\nu_\phi - \nu_r$ ,  $\nu_L = 2(\nu_\phi - \nu_r)$ .

Figure 13 illustrates the relations between the upper and lower frequencies of twin-peak QPOs for different models of BHs and QPOs. In the numerical calculations, for simplicity we have considered the stellar mass BHs. One can easily see from the top right panel in Fig. 13 that WD models could explain the existence of high-frequency QPOs (up to 900–1000 Hz) for the Schwarzschild case and the regular nonminimal BH at higher values of the coupling parameter of the YM field. The RP and ER2–ER4 models could explain QPO frequencies up to  $\sim 430$  Hz. In Fig. 13 the area between gray and black dotted (blue dot-dashed, red dashed) lines implies the possible values of frequency of twin-peak QPOs from rotating Kerr (RN, nonminimal regular) BHs. From this point of view the QPO objects can be modeled by all of the considered BHs. In other words, the observation of such QPOs cannot distinguish the types of BH. Our numerical analysis shows that the RN BH charge can mimic the spin of the Kerr BH up to  $a/M \simeq 0.51$ , and the nonminimal regular magnetic BH up to  $a/M \simeq 0.215$  at  $q = 1$  in the RP model.

One of the important feature of the above analysis is that it may be helpful to distinguish between the gravity models describing the central QPO object. In other words, if the position of a twin-peak QPO corresponding to the  $\nu_U - \nu_L$  space shown in Fig. 13 is located between the black dotted and blue dot-dashed lines, the central BH can be a rotating Kerr one. However, if the position QPO is located in the space between the blue dot-dashed and red dashed lines, then the central BH can be either the RN or the Kerr one. Similar scenarios may appear when the position of the QPO lies between the red dashed and the gray solid lines: one

cannot distinguish whether the central object is the rotating Kerr, RN, or nonminimal regular magnetic BH with the coupling parameter  $q \geq 1$ .

## V. CONCLUSION

In this work, we have studied the spacetime properties around a regular nonminimal magnetic BH. We have also analyzed the dynamics of neutral, magnetized, and magnetically charged particles around a central object. The main results of the paper can be summarized as follows:

- (i) Our analysis shows that the maximum values of the curvature invariants decrease with an increase in the nonminimal coupling parameter. The minimal outer horizon corresponding to the extreme value of charge BH increases with an increase in the coupling parameter and reaches its maximum  $1.5M$  when  $q \rightarrow \infty$ . On the other hand, the maximum value of the charge of the BH decreases tends to zero with an increase in parameter  $q$ .
- (ii) The studies of test particle motion have shown that the ISCO radius decreases with an increase in the magnetic charge of the nonminimal regular magnetic BH. With an increase in the coupling parameter the ISCO radius increases due to a decrease in the extreme value of the BH charge. It has also been shown that when the parameter  $q$  tends to infinity the ISCO radius tends to the value  $r_{\text{ISCO}} \rightarrow 4.5M$ .
- (iii) We have explored the cases where, due to the effects of the magnetic charge parameter and the spin of the rotating Kerr BH, particles have the same ISCO radius. It has been shown that the mimicked values of the spin parameter decrease with an increase in the coupling parameters.
- (iv) The studies of the effects of the magnetic charge of the nonminimal regular BH and the coupling parameters on the energy efficiency have shown that an increase in the coupling parameter causes a decrease in the efficiency of the energy extraction.
- (v) We have also studied the fundamental frequencies around the nonminimal magnetic BHs in comparison to those around the Schwarzschild, RN, and Kerr BHs. The studies have shown that an increase in the coupling parameter of the YM field causes a decrease in the Keplerian and radial frequencies. On the other hand, an increase in the charge of both the RN and nonminimal magnetic BHs increases the epicyclic frequencies.
- (vi) We have also explored the relations of upper and lower frequencies of twin-peak QPO around the magnetic, RN Schwarzschild, and Kerr BHs for different QPO models. Our analysis has shown that the RN BH charge can mimic the spin of a Kerr BH up to  $a/M \simeq 0.51$ , and a nonminimal regular magnetic BH up to  $a/M \simeq 0.215$  at  $q = 1$  in the RP model.

## ACKNOWLEDGMENTS

The authors thank Bobur Turimov for the useful discussions. A. A. acknowledges the support of the PIFI fund of the Chinese Academy of Sciences. J. R. acknowledges

the support of SPACECOM through ERASMUS+Project No. 608715-EPP-1-2019-1-UZ-EPPKA2-JP. W.-B. H is supported by NSFC (National Natural Science Foundation of China) Grant No. 11773059.

- 
- [1] R. J. Scherrer, *Phys. Rev. Lett.* **93**, 011301 (2004).
- [2] P. Jordan, *Nachr. Akad. Wiss. Goettingen* **2** **1945**, 39 (1945), <https://ui.adsabs.harvard.edu/abs/1945PA.....53.251J>.
- [3] C. Brans and R. H. Dicke, *Phys. Rev.* **124**, 925 (1961).
- [4] H. Goenner, *Gen. Relativ. Gravit.* **44**, 2077 (2012).
- [5] C. G. Callan, Jr., S. Coleman, and R. Jackiw, *Ann. Phys. (N.Y.)* **59**, 42 (1970).
- [6] V. Faraoni, E. Gunzig, and P. Nardone, *Fundam. Cosm. Phys.* **20**, 121 (1999), <https://ui.adsabs.harvard.edu/abs/1999FCPh..20..121>.
- [7] A. R. Prasanna, *Phys. Lett.* **37A**, 331 (1971).
- [8] I. T. Drummond and S. J. Hathrell, *Phys. Rev. D* **22**, 343 (1980).
- [9] F. W. Hehl and Y. N. Obukhov, in *Gyros, Clocks, Interferometers ...: Testing Relativistic Gravity in Space*, Lecture Notes in Physics Vol. 562, edited by C. Lämmerzahl, C. W. F. Everitt, and F. W. Hehl (Springer, New York, 2001), p. 479.
- [10] A. B. Balakin and J. P. S. Lemos, *Classical Quantum Gravity* **22**, 1867 (2005).
- [11] G. W. Horndeski, *Arch. Ration. Mech. Anal.* **75**, 229 (1981).
- [12] A. B. Balakin, H. Dehnen, and A. E. Zayats, *Phys. Rev. D* **76**, 124011 (2007).
- [13] A. B. Balakin, H. Dehnen, and A. E. Zayats, *Int. J. Mod. Phys. D* **17**, 1255 (2008).
- [14] A. B. Balakin and W.-T. Ni, *Classical Quantum Gravity* **27**, 055003 (2010).
- [15] G. W. Horndeski, *Phys. Rev. D* **17**, 391 (1978).
- [16] F. Muller-Hoissen and R. Sippel, *Classical Quantum Gravity* **5**, 1473 (1988).
- [17] A. B. Balakin, S. V. Sushkov, and A. E. Zayats, *Phys. Rev. D* **75**, 084042 (2007).
- [18] A. B. Balakin, J. P. S. Lemos, and A. E. Zayats, *Phys. Rev. D* **81**, 084015 (2010).
- [19] A. B. Balakin and A. E. Zayats, *Phys. Rev. D* **90**, 044049 (2014).
- [20] A. B. Balakin, V. V. Bochkarev, and J. P. S. Lemos, *Phys. Rev. D* **77**, 084013 (2008).
- [21] A. B. Balakin and A. E. Zayats, *Int. J. Mod. Phys. D* **24**, 1542009 (2015).
- [22] A. B. Balakin and A. E. Zayats, *Phys. Lett. B* **644**, 294 (2007).
- [23] J. A. Smoller, A. G. Wasserman, and S. T. Yau, *Commun. Math. Phys.* **154**, 377 (1993).
- [24] M. S. Volkov and N. Straumann, *Phys. Rev. Lett.* **79**, 1428 (1997).
- [25] B. Kleihaus and J. Kunz, *Phys. Rev. Lett.* **86**, 3704 (2001).
- [26] B. Kleihaus, J. Kunz, and F. Navarro-Lérida, *Phys. Rev. D* **66**, 104001 (2002).
- [27] S. G. Ghosh and N. Dadhich, *Phys. Rev. D* **82**, 044038 (2010).
- [28] T. Moon, Y. S. Myung, and E. J. Son, *Gen. Relativ. Gravit.* **43**, 3079 (2011).
- [29] J. A. R. Cembranos and J. G. Valcarcel, *Eur. Phys. J. C* **77**, 853 (2017).
- [30] M. Prottar and A. DeBenedictis, *Phys. Rev. D* **97**, 106009 (2018).
- [31] A. B. Balakin, J. P. S. Lemos, and A. E. Zayats, *Phys. Rev. D* **93**, 024008 (2016).
- [32] K. Jusufi, M. Azreg-Aïnou, M. Jamil, S.-W. Wei, Q. Wu, and A. Wang, *Phys. Rev. D* **103**, 024013 (2021).
- [33] R. M. Wald, *Phys. Rev. D* **10**, 1680 (1974).
- [34] S. Chen, M. Wang, and J. Jing, *J. High Energy Phys.* **09** (2016) 082.
- [35] K. Hashimoto and N. Tanahashi, *Phys. Rev. D* **95**, 024007 (2017).
- [36] S. Dalui, B. R. Majhi, and P. Mishra, *Phys. Lett. B* **788**, 486 (2019).
- [37] W. Han, *Gen. Relativ. Gravit.* **40**, 1831 (2008).
- [38] A. P. S. de Moura and P. S. Letelier, *Phys. Rev. E* **61**, 6506 (2000).
- [39] V. S. Morozova, L. Rezzolla, and B. J. Ahmedov, *Phys. Rev. D* **89**, 104030 (2014).
- [40] Z. Stuchlík, M. Kološ, J. Kovář, P. Slaný, and A. Tursunov, *Universe* **6**, 26 (2020).
- [41] A. Jawad, F. Ali, M. Jamil, and U. Debnath, *Commun. Theor. Phys.* **66**, 509 (2016).
- [42] S. Hussain and M. Jamil, *Phys. Rev. D* **92**, 043008 (2015).
- [43] M. Jamil, S. Hussain, and B. Majeed, *Eur. Phys. J. C* **75**, 24 (2015).
- [44] S. Hussain, I. Hussain, and M. Jamil, *Eur. Phys. J. C* **74**, 3210 (2014).
- [45] G. Z. Babar, M. Jamil, and Y.-K. Lim, *Int. J. Mod. Phys. D* **25**, 1650024 (2016).
- [46] M. Bañados, J. Silk, and S. M. West, *Phys. Rev. Lett.* **103**, 111102 (2009).
- [47] B. Majeed and M. Jamil, *Int. J. Mod. Phys. D* **26**, 1741017 (2017).
- [48] A. Zakria and M. Jamil, *J. High Energy Phys.* **05** (2015) 147.
- [49] I. Brevik and M. Jamil, *Int. J. Geom. Methods Mod. Phys.* **16**, 1950030 (2019).
- [50] M. De Laurentis, Z. Younsi, O. Porth, Y. Mizuno, and L. Rezzolla, *Phys. Rev. D* **97**, 104024 (2018).

- [51] S. R. Shaymatov, B. J. Ahmedov, and A. A. Abdujabbarov, *Phys. Rev. D* **88**, 024016 (2013).
- [52] F. Atamurotov, B. Ahmedov, and S. Shaymatov, *Astrophys. Space Sci.* **347**, 277 (2013).
- [53] M. Kološ, A. Tursunov, and Z. Stuchlík, *Eur. Phys. J. C* **77**, 860 (2017).
- [54] J. Kovář, O. Kopáček, V. Karas, and Z. Stuchlík, *Classical Quantum Gravity* **27**, 135006 (2010).
- [55] J. Kovář, P. Slaný, C. Cremașchini, Z. Stuchlík, V. Karas, and A. Trova, *Phys. Rev. D* **90**, 044029 (2014).
- [56] A. N. Aliev and D. V. Gal'tsov, *Sov. Phys. Usp.* **32**, 75 (1989).
- [57] A. N. Aliev and N. Özdemir, *Mon. Not. R. Astron. Soc.* **336**, 241 (2002).
- [58] A. N. Aliev, D. V. Gal'tsov, and V. I. Petukhov, *Astrophys. Space Sci.* **124**, 137 (1986).
- [59] V. P. Frolov and P. Krtouš, *Phys. Rev. D* **83**, 024016 (2011).
- [60] V. P. Frolov, *Phys. Rev. D* **85**, 024020 (2012).
- [61] Z. Stuchlík, J. Schee, and A. Abdujabbarov, *Phys. Rev. D* **89**, 104048 (2014).
- [62] S. Shaymatov, F. Atamurotov, and B. Ahmedov, *Astrophys. Space Sci.* **350**, 413 (2014).
- [63] A. Abdujabbarov and B. Ahmedov, *Phys. Rev. D* **81**, 044022 (2010).
- [64] A. Abdujabbarov, B. Ahmedov, and A. Hakimov, *Phys. Rev. D* **83**, 044053 (2011).
- [65] A. A. Abdujabbarov, B. J. Ahmedov, S. R. Shaymatov, and A. S. Rakhmatov, *Astrophys. Space Sci.* **334**, 237 (2011).
- [66] A. A. Abdujabbarov, B. J. Ahmedov, and V. G. Kagramanova, *Gen. Relativ. Gravit.* **40**, 2515 (2008).
- [67] S. Shaymatov, M. Patil, B. Ahmedov, and P. S. Joshi, *Phys. Rev. D* **91**, 064025 (2015).
- [68] J. Rayimbaev, B. Turimov, F. Marcos, S. Palvanov, and A. Rakhmatov, *Mod. Phys. Lett. A* **35**, 2050056 (2020).
- [69] B. Turimov, B. Ahmedov, A. Abdujabbarov, and C. Bambi, *Phys. Rev. D* **97**, 124005 (2018).
- [70] B. V. Turimov, B. J. Ahmedov, and A. A. Hakimov, *Phys. Rev. D* **96**, 104001 (2017).
- [71] S. Shaymatov, J. Vrba, D. Malafarina, B. Ahmedov, and Z. Stuchlík, *Phys. Dark Universe* **30**, 100648 (2020).
- [72] J. R. Rayimbaev, B. J. Ahmedov, N. B. Juraeva, and A. S. Rakhmatov, *Astrophys. Space Sci.* **356**, 301 (2015).
- [73] S. Shaymatov, *Int. J. Mod. Phys. Conf. Ser.* **49**, 1960020 (2019).
- [74] J. Rayimbaev, B. Turimov, and B. Ahmedov, *Int. J. Mod. Phys. D* **28**, 1950128 (2019).
- [75] S. Shaymatov, D. Malafarina, and B. Ahmedov, *arXiv: 2004.06811*.
- [76] B. Narzilloev, A. Abdujabbarov, C. Bambi, and B. Ahmedov, *Phys. Rev. D* **99**, 104009 (2019).
- [77] B. Narzilloev, D. Malafarina, A. Abdujabbarov, and C. Bambi, *Eur. Phys. J. C* **80**, 784 (2020).
- [78] B. Narzilloev, J. Rayimbaev, A. Abdujabbarov, and C. Bambi, *Eur. Phys. J. C* **80**, 1074 (2020).
- [79] B. Narzilloev, J. Rayimbaev, S. Shaymatov, A. Abdujabbarov, B. Ahmedov, and C. Bambi, *Phys. Rev. D* **102**, 044013 (2020).
- [80] B. Narzilloev, J. Rayimbaev, S. Shaymatov, A. Abdujabbarov, B. Ahmedov, and C. Bambi, *Phys. Rev. D* **102**, 104062 (2020).
- [81] F. de Felice and F. Sorge, *Classical Quantum Gravity* **20**, 469 (2003).
- [82] F. de Felice, F. Sorge, and S. Zilio, *Classical Quantum Gravity* **21**, 961 (2004).
- [83] J. R. Rayimbaev, *Astrophys. Space Sci.* **361**, 288 (2016).
- [84] T. Oteev, A. Abdujabbarov, Z. Stuchlík, and B. Ahmedov, *Astrophys. Space Sci.* **361**, 269 (2016).
- [85] B. Toshmatov, A. Abdujabbarov, B. Ahmedov, and Z. Stuchlík, *Astrophys. Space Sci.* **360**, 19 (2015).
- [86] A. Abdujabbarov, B. Ahmedov, O. Rahimov, and U. Salikhbaev, *Phys. Scr.* **89**, 084008 (2014).
- [87] O. G. Rahimov, A. A. Abdujabbarov, and B. J. Ahmedov, *Astrophys. Space Sci.* **335**, 499 (2011).
- [88] O. G. Rahimov, *Mod. Phys. Lett. A* **26**, 399 (2011).
- [89] K. Haydarov, A. Abdujabbarov, J. Rayimbaev, and B. Ahmedov, *Universe* **6**, 44 (2020).
- [90] K. Haydarov, J. Rayimbaev, A. Abdujabbarov, S. Palvanov, and D. Begmatova, *Eur. Phys. J. C* **80**, 399 (2020).
- [91] J. Rayimbaev, A. Abdujabbarov, M. Jamil, B. Ahmedov, and W.-B. Han, *Phys. Rev. D* **102**, 084016 (2020).
- [92] J. Rayimbaev, M. Figueroa, Z. Stuchlík, and B. Juraev, *Phys. Rev. D* **101**, 104045 (2020).
- [93] J. Vrba, A. Abdujabbarov, M. Kološ, B. Ahmedov, Z. Stuchlík, and J. Rayimbaev, *Phys. Rev. D* **101**, 124039 (2020).
- [94] A. Abdujabbarov, J. Rayimbaev, B. Turimov, and F. Atamurotov, *Phys. Dark Universe* **30**, 100715 (2020).
- [95] B. Turimov, J. Rayimbaev, A. Abdujabbarov, B. Ahmedov, and Z. C. V. Stuchlík, *Phys. Rev. D* **102**, 064052 (2020).
- [96] A. H. Bokhari, J. Rayimbaev, and B. Ahmedov, *Phys. Rev. D* **102**, 124078 (2020).
- [97] N. Juraeva, J. Rayimbaev, A. Abdujabbarov, B. Ahmedov, and S. Palvanov, *Eur. Phys. J. C* **81**, 70 (2021).
- [98] L. Angelini, L. Stella, and A. N. Parmar, *Astrophys. J.* **346**, 906 (1989).
- [99] M. A. Abramowicz, A. Lanza, E. A. Spiegel, and E. Szuszkiewicz, *Nature (London)* **356**, 41 (1992).
- [100] L. Stella and M. Vietri, *Astrophys. J. Lett.* **492**, L59 (1998).
- [101] A. Čadež, M. Calvani, and U. Kostić, *Astron. Astrophys.* **487**, 527 (2008).
- [102] U. Kostić, A. Čadež, M. Calvani, and A. Gomboc, *Astrophys. Astron.* **496**, 307 (2009).
- [103] M. A. Abramowicz and W. Kluźniak, *Astron. Astrophys.* **374**, L19 (2001).
- [104] P. Bakala, G. Török, V. Karas, M. Dovčiak, M. Wildner, D. Wzientek, E. Šrámková, M. Abramowicz, K. Goluchová, G. P. Mazur, and F. H. Vincent, *Mon. Not. R. Astron. Soc.* **439**, 1933 (2014).
- [105] G. D. KarsSEN, M. Bursa, A. Eckart, M. Valencia-S., M. Dovčiak, V. Karas, and J. Horák, *Mon. Not. R. Astron. Soc.* **472**, 4422 (2017).
- [106] C. Germanà, *Phys. Rev. D* **96**, 103015 (2017).
- [107] S. Kato and J. Fukue, *Publ. Astron. Soc. Jpn.* **60**, 377 (1980).
- [108] A. T. Okazaki, S. Kato, and J. Fukue, *Publ. Astron. Soc. Jpn.* **39**, 457 (1987), <https://ui.adsabs.harvard.edu/abs/1987PASJ...39..457O>.

- [109] M. A. Nowak and R. V. Wagoner, *Astrophys. J.* **393**, 697 (1992).
- [110] R. V. Wagoner, *Phys. Rep.* **311**, 259 (1999).
- [111] R. V. Wagoner, A. S. Silbergleit, and M. Ortega-Rodríguez, *Astrophys. J. Lett.* **559**, L25 (2001).
- [112] A. S. Silbergleit, R. V. Wagoner, and M. Ortega-Rodríguez, *Astrophys. J.* **548**, 335 (2001).
- [113] D. H. Wang, L. Chen, C. M. Zhang, Y. J. Lei, J. L. Qu, and L. M. Song, *Mon. Not. R. Astron. Soc.* **454**, 1231 (2015).
- [114] L. Rezzolla, S. Yoshida, T. J. Maccarone, and O. Zanotti, *Mon. Not. R. Astron. Soc.* **344**, L37 (2003).
- [115] G. Török and Z. Stuchlík, *Astron. Astrophys.* **437**, 775 (2005).
- [116] A. Ingram and C. Done, *Mon. Not. R. Astron. Soc.* **405**, 2447 (2010).
- [117] P. C. Fragile, O. Straub, and O. Blaes, *Mon. Not. R. Astron. Soc.* **461**, 1356 (2016).
- [118] Z. Stuchlík, A. Kotrlová, and G. Török, *Astron. Astrophys.* **552**, A10 (2013).
- [119] Z. Stuchlík, A. Kotrlová, and G. Török, *Acta Astron.* **62**, 389 (2012), <https://ui.adsabs.harvard.edu/abs/2012AcA...62..389S>.
- [120] M. Ortega-Rodríguez, H. Solís-Sánchez, L. Álvarez-García, and E. Dodero-Rojas, *Mon. Not. R. Astron. Soc.* **492**, 1755 (2020).
- [121] A. Maselli, G. Pappas, P. Pani, L. Gualtieri, S. Motta, V. Ferrari, and L. Stella, *Astrophys. J.* **899**, 139 (2020).
- [122] J. M. Bardeen, W. H. Press, and S. A. Teukolsky, *Astrophys. J.* **178**, 347 (1972).
- [123] I. D. Novikov and K. S. Thorne, in *Black Holes (Les Astres Occlus)*, edited by C. Dewitt and B. S. Dewitt (Gordon & Breach, New York, 1973), pp. 343–450.
- [124] G. Török, *Astron. Astrophys.* **440**, 1 (2005).
- [125] Z. Stuchlík and J. Schee, *Classical Quantum Gravity* **29**, 065002 (2012).
- [126] Z. Stuchlík and M. Kološ, *Astron. Astrophys.* **586**, A130 (2016).
- [127] L. Stella, M. Vietri, and S. M. Morsink, *Astrophys. J.* **524**, L63 (1999).
- [128] S. Kato, *Publ. Astron. Soc. Jpn.* **56**, 905 (2004).
- [129] S. Kato, *Publ. Astron. Soc. Jpn.* **60**, 889 (2008).

*Correction:* The name of the last author appeared incorrectly owing to a database error and has been fixed.